Ahmed Abed[1], Nick Thom[1], and Luis Neves[1]

[1]*Nottingham Transportation Engineering Centre, the University of Nottingham, Nottingham, UK.*

Corresponding author: Ahmed Abed

Email address: ahmed.abed@nottingham.ac.uk

Nick Thom

nicholas.thom@nottingham.ac.uk

Luis Neves

Luis.Neves@nottingham.ac.uk

Abstract

Variability of pavement design parameters has always been a concern to pavement designers and highway agencies. A robust pavement design should take into account the variability of the design inputs and its impact on the reliability of the design. In this study, the variability effect of thickness and stiffness of pavement layers was investigated. The variability of these parameters was described by their mean values, standard deviations and probability distribution functions. Monte Carlo Simulation method was utilised to incorporate variability of the design parameters and to construct the probability distribution function of the outputs. KENLAYER software was used to calculate pavement response at predetermined critical locations; pavement reponse was then used to predict pavement performance regarding permanent deformation, bottom-up and top-down fatigue cracking by using the mechanistic empirical pavement design guide (MEPDG) models. A Matlab code was developed to run that analysis and obtain the probability distribution function of pavement performance indicators over time. It was found that the variability of pavement layer thickness and stiffness has a significant impact on pavement performance. Also, it was found that not only the mean of the predicted performance indicators is increasing over time, but the variance of these indicators is also increasing. This means that pavement condition cannot be described by the mean values of the indicators but by the probability distribution function which can describe pavement condition at any reliability level.

1

Introduction

The concept of incorporating variability of pavement design variables in pavement analysis and design was first introduced by Darter and Hudson (1973). They stated that due to the stochastic nature of pavement design parameters, a probabilistic design approach that takes into account the inherent variability and uncertainty of those parameters must be implemented in order to improve the reliability of the pavement design process. They also developed a design model that calculates the reliability of the design as the probability that the number of load application that the pavement can sustain is larger than the expected number of load application. Despite that their work was limited to the effect of variability of pavement design parameters on pavement serviceability loss due to traffic loading, it can be considered as the basis for the probabilistic pavement design because it became possible for pavement engineers to design the pavement based on a certain level of reliability. Later, the reliability principle was included as a part of AASHTO (1986) and AASHTO (1993) design guides; it was defined as the degree of certainty that a pavement designer adds to assure that the designed pavement maintains a certain level of serviceability over the design period. Such as $ESAL_R=ESAL_{50\%}+SE \times ZR$ where $ESAL_{50\%}$ is the predicted number of load application at 50% reliability, SE is the standard error, ZR is the standard normal deviate, and $ESAL_R$ is the predicted number of load application based on the desired reliability level. Therefore, a reliability factor that can be selected based on the road type was developed which merely meant to assure that the designed Equivalent Single Axle Load (ESAL) exceeds the expected ESAL.

In a similar reliability analysis approach, the Mechanistic-Empirical Pavement Design Guide (MEPDG) (NCHRP, 2004a) included the effect of variability of pavement design parameters on the design process; but this time the variability was considered by its impact on the predicted pavement distresses rather than the expected ESAL. The variability effect was evaluated by calculating the standard error between the predicted distresses via MEPDG models and the observed distress from

2

real pavement sections, and calibration factors were suggested to minimise the perdition error. The benefit of this approach is that pavement designers can evaluate the variability impact on every pavement distress, which can be quite useful in understanding the sensitivity of the distress against the variability of the design inputs. Hence identifying the critical design parameters to design against certain dominant distress types.

Generally, pavement performance prediction can be either deterministic or probabilistic (Amador-Jiménez and Mrawira, 2011; Wang, Zaniewski, & Way, 1994). The deterministic prediction can be divided into three models, mechanistic, empirical, or mechanistic-empirical (M-E). A detailed discussion regarding these models can be found elsewhere (K. A. Abaza, 2004; Collop and Cebon, 1995; George, Rajagopal, & Lim, 1989). The main drawback with these models is the incapability of these models to address input dispersions thus only the mean value of the studied indicator is obtained after the analysis (Valle, 2015). Furthermore, to improve the reliability of the deterministic methods, the designers apply safety factors based on engineering judgment which may result in either "overdesign" or "underdesign" problems (Huang, 2004). On the other hand, the probabilistic prediction requires previous knowledge of the design input distributions to obtain a distribution rather than a definite value of the analysed indicator. This approach has been suggested to include uncertainty associated with the design inputs to improve design reliability (K. A. Abaza, 2014; Butt, Shahin, Feighan, & Carpenter, 1987; Hassan, Lin, & Thananjeyan, 2015; Li, Haas, & Xie, 1996; Wang, et al., 1994). Most of these studies, however, have implemented Markov Chain to predict the future condition of the pavement based on the previous conditions. The application of Markov chain requires historical quality data regarding pavement condition such as assessment of distress at least two different times in order to calculate Markov Chain transition matrix which is the central element to predict the future state of the pavement. However, these data may not always be available. Moreover, pavement condition prediction is performed purely based on surface distress

3

assessment. Thus the underlying mechanism that causing pavement deterioration is not included in this analysis. In other words, pavement mechanical properties which are the main factors in predicting the distress, are not involved in the prediction process. Furthermore, using the same transition matrix to predict pavement future condition may not be realistic since pavement deterioration rate may not be constant. Accordingly, some researchers suggested using a non-homogeneous Markov Chain to address this issue (K. Abaza and Murad, 2007; K. A. Abaza, 2015). In contrast, a different transition matrix has to be used to predict future pavement condition for every period of performance. However, at the end of every analysis period, the transition matrix has to be calibrated based on the difference between the predicted and the actual pavement condition.

One of the interesting techniques in risk analysis studies is Monte Carlo (MC) simulation method. The concept of this method is to probabilistically predict the performance of a system by randomly generating a set of inputs according to their probability distribution functions, then using analytical models that link the inputs with the outputs to predict the system behaviour; running the model for many simulations results in several predictions of the system performance, the predictions can then be used to establish the probability distribution of the output (Ayyub and Klir, 2006). In pavement engineering applications, Xiao (2012) applied MC method to analysing and improving the reliability of the MEPDG model. He developed a probabilistic design tool that was able to evaluate the reliability of pavement design process. However, based on approximation techniques such as the equivalent thickness and surface response methods, he developed a surrogate model to predict pavement response and smoothness. This means that pavement stress and strain were calculated based on an approximate solution rather than the exact solution of the multilayer elastic system which may affect the accuracy of the simulation process. Wu, Yang, & Sun (2017) applied MC filtration method to run a sensitivity analysis to the MEPDG. They demonstrated that this method could be a valuable tool to identify the significant pavement design parameters, they also observed

4

that 350 simulations were required to rank the critical and important parameters. The simulation time, however, was relatively high, it took about fifty hours to simulate fifteen years five hundred times.

Despite the approach that is implemented to address the reliability of pavement design, we have to consider that there is significant variability in pavement design parameters that have to be taken into account in the design process. Table 1 (Valle, 2015) presents a summary of the variability associated with the design primary input parameters expressed by the Coefficient of Variations (CoV) and the probability distribution function of those parameters. This table provides an obvious idea of the level of variability exists in the thickness and stiffness of pavement layers which are the main pavement design input parameters. The thickness of the bituminous layers can vary 7-10%, whereas it can vary 12-15% for the granular layers, whereas the stiffness can vary 10-20% for the bituminous layers and 10-30% for the unbound pavement layers. This level of variability can significantly affect the accuracy and reliability of the predicted pavement performance. Accordingly, this study aims to develop a probabilistic performance prediction tool that considers the variability of the design parameters in the prediction process by the application of MC method.

Table 1. Pavement layer thickness and stiffness variations and their suggested probability distributions (Valle, 2015)

Property	Description	Range CoV %	Typical CoV%	Type of distribution	Reference
Layer thickness	Bituminous surface	3-12	7	Normal	Timm et al. (2000), Noureldin et al. (1994)
		3.2-18.4	7.2	Normal	Aguiar-Moya et al. (2009)
	Bituminous binder course	11.7-16	13.8	Normal	Aguiar-Moya et al. (2009)
		5-15	10	Normal	Noureldin et al. (1994)
	Granular base	10-15	12	Normal	Noureldin et al. (1994)
		6-17.2	10.3	Normal	Noureldin et al. (1994)
	Granular subbase	10-20	15	Normal	Noureldin et al. (1994)
Elastic modulus	Bituminous layers	10-20	15	Normal	Noureldin et al. (1994)
		10-40		Lognormal	Timm et al. (2000)
	Granular base	10-30	20	Normal	Noureldin et al. (1994)
		5-60		Lognormal	Timm et al. (2000)
	Granular subbase	10-30	20	Normal	Noureldin et al. (1994)
		5-60		Lognormal	Timm et al. (2000)
	Granular subgrade	10-30	20	Normal	Noureldin et al. (1994)
		20-45		Lognormal	Timm et al. (2000)

Model Development

The model developed in this study is graphically represented in Figure 1. Firstly, the model generates random design variables based on their mean values and their probability distribution functions. Secondly, it sends the generated values to Kenlayer software to calculate pavement

6

response (strains) at predefined critical locations. Finally, it uses M-E models to predict pavement distress, which were: bottom-up fatigue cracking, top-down fatigue cracking, and permanent deformation. The critical strains considered in this study were: the horizontal tensile strain at the bottom of the base layer to predict bottom-up fatigue cracking, the horizontal tensile strain at the pavement surface to predict top-down fatigue cracking, and the vertical compressive strain at the middle of each of pavement layers to predict the permanent deformation. To demonstrate the application of the suggested model, a typical pavement structure as shown in Figure 2 has been considered in this study. The following sections explain the details of the developed model.

Thickness of Pavement Layers

To introduce variability effect of this parameter, the recommended thickness coefficients of variation reported in Table 1 were implemented. The thickness of pavement layers was assumed to be normally distributed. The mean thickness values are as shown in Figure 2, whereas the standard deviation can be calculated by multiplying the CoV by the mean values. After determining the mean and the standard deviation of the layer thickness, random thickness values of each layer were generated by MC method. Figure 3 presents the distributions of the generated values.
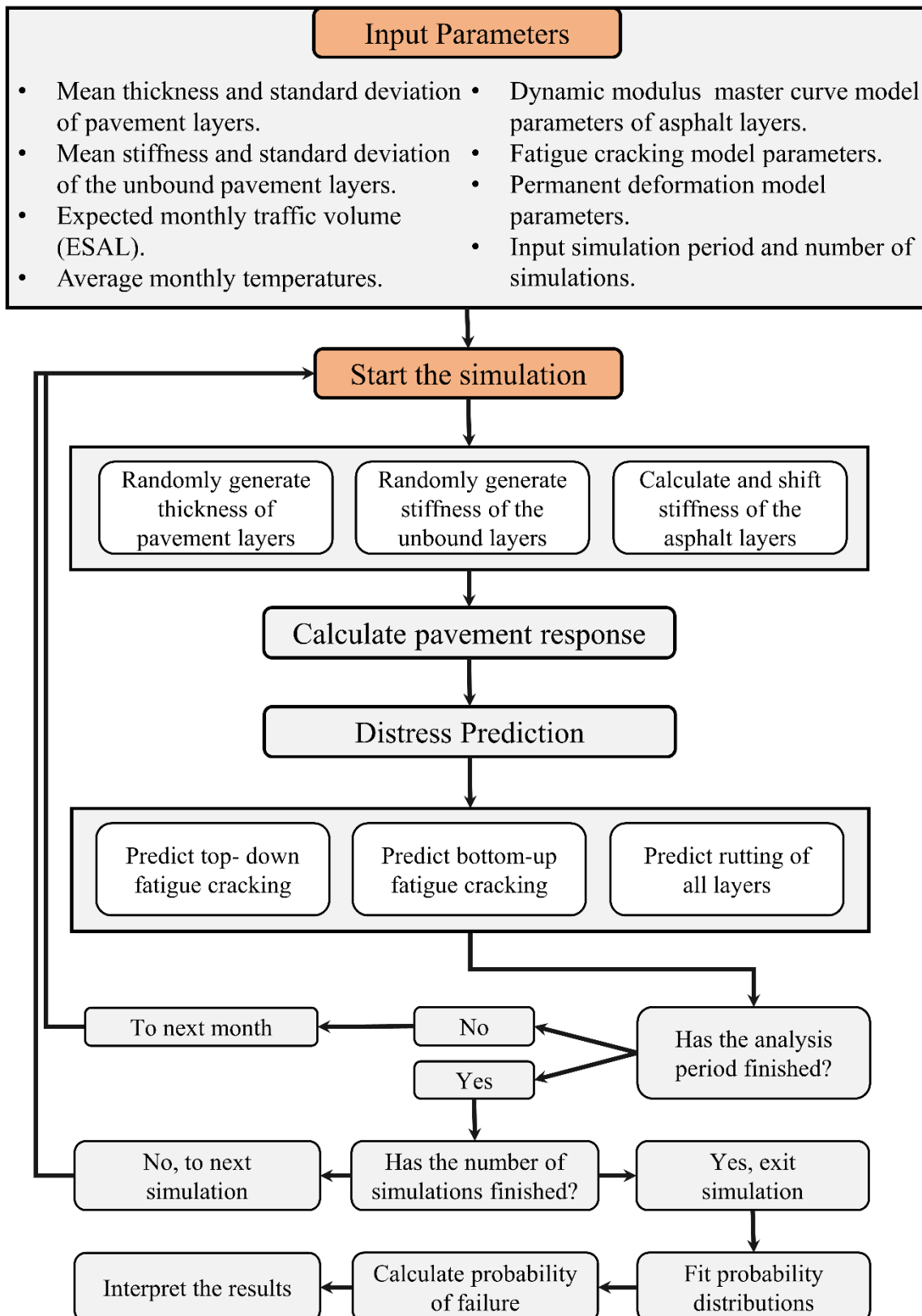
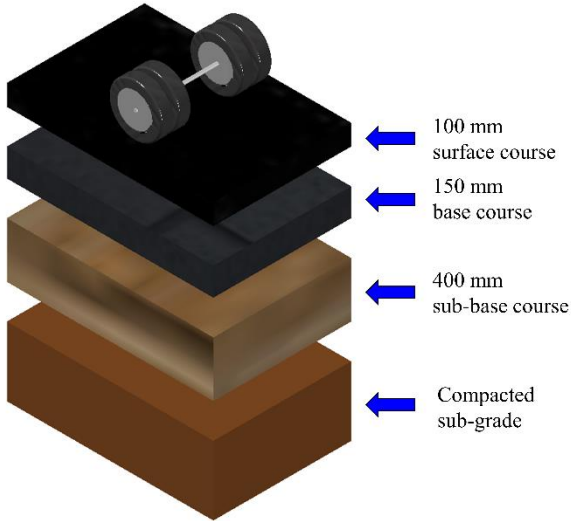Figure 1. Flowchart of the simulation model
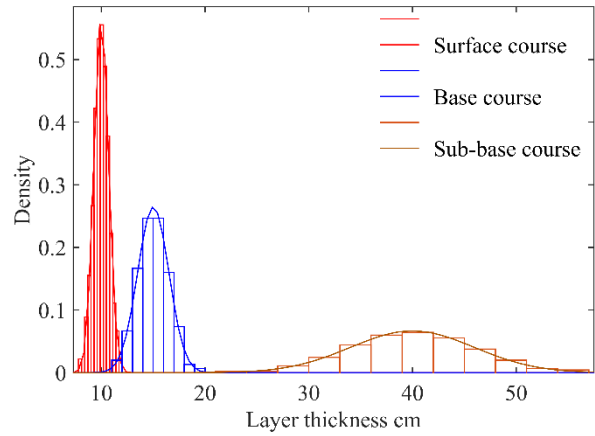
Figure 2. Four-layer pavement

Figure 3. Thickness of pavement layers

Pavement Temperature

Pavement temperature is one of the significant inputs to calculate the dynamic modulus of the

asphaltic materials (Y. R. Kim, Underwood, Far, Jackson, & Puccinelli, 2011). To accurately

compute pavement response, it is necessary that pavement temperature at the time of the analysis be

defined so that the dynamic modulus can be calculated accordingly. Pavement temperature is

usually determined from air temperature data which can be collected from weather stations, and

several available regression models to calculate pavement temperature can be found in the

literature. The model implemented in this study is the one that was reported by Mohseni (1998) as

follows:

$$\text{Temp}_{\text{pav-low}} = -1.56 + 0.72 \times T_{air} - 0.004 \times Lat^2 + 6.26 \log_{10}(H + 25) \qquad \text{Equation 1}$$

$$\text{Temp}_{\text{pav-high}} = 54.32 + 0.78 \times T_{air} - 0.0025 \times Lat^2 - 15.14 \log_{10}(H + 25) \qquad \text{Equation 2}$$

where $\text{Temp}_{\text{pav-low}}$ is the low pavement temperature °C, $\text{Temp}_{\text{pav-high}}$ is the high pavement

temperature, T_{air} air temperature °C, Lat is the latitude of the section degrees, and H is the depth to

9

pavement surface mm. These models result in two pavement temperatures; one is lower, and one is higher than the air temperature. If the air temperature is rising, then the pavement is absorbing energy and pavement temperature is lower than the air temperature; if the air temperature is dropping, then the pavement is emitting energy and the pavement temperature is higher than the air temperature. Accordingly, for the same air temperature there are different possible pavement temperatures, one is lower, one is higher than the air temperature, and the third one is an average of the low and high pavement temperatures.

Furthermore, these models require only air temperature data and the latitude of the analysed section to calculate pavement temperature. However, to calculate the air temperature at any time, it is necessary to model the air temperature as a function of time. Since the air temperature periodically changes over time, then it is logical to assume that the air temperature can be modelled as a sine wave of time. To prove this assumption, local weather data of Nottingham city for the past forty years was downloaded from UK Forecast (2019) website and implemented in this study. The average monthly temperature was then predicted using the following trigonometric function:

$$\text{Temp}_{\text{time}} = \text{AMT} + \frac{\text{MaxT} - \text{MinT}}{2} \times \sin(2\pi \times \frac{Tm}{12} + \theta) \qquad \text{Equation 3}$$

where $\text{Temp}_{\text{time}}$ is the predicted temperature as a function of time, AMT is the average monthly temperature, MaxT is the maximum temperature, MinT is the minimum temperature, Tm is the time in months, and θ is a shit angle to fit the sine wave with temperature data. The optimisation function "SOLVER" embedded in Excel software was used to calculate model parameters; a sample of the real data and the predicted air temperatures and pavement temperatures as well are presented in Figure 4. This figure shows that the predicted average monthly temperature fits very well with the measured average monthly temperatures. It also shows that monthly air

10

temperatures can result in three pavement temperatures; low and high pavement temperatures that are calculated based on Equation 1 and Equation 2, and an average of these temperatures. The low pavement temperature represents pavement temperatures at night and early morning times; the high pavement temperature represents pavement temperatures at the noon and afternoon times; whereas the average pavement temperature represents pavement temperatures between early morning and noon times. Based on this assumption, the entire spectrum of pavement temperatures can be represented, and the pavement damage at each of these temperatures can be predicted and accumulated in the analysis. Traffic volume of every month was then divided into three parts, 10% at the low pavement temperature, 70% at average pavement temperature, and 20% at the high pavement temperature. This assumption may approximately match traffic hourly distribution with temperature hourly distribution, but it is necessary to account for pavement damage that is accumulated at different temperatures and traffic volumes. Furthermore, this procedure should improve the damage prediction process because the damage in this case is calculated based on traffic damage and pavement temperatures when the traffic is passing. Certainly, pavement temperatures can be divided more finely and different traffic volumes can be assigned to each part, but this can be a time-consuming process.
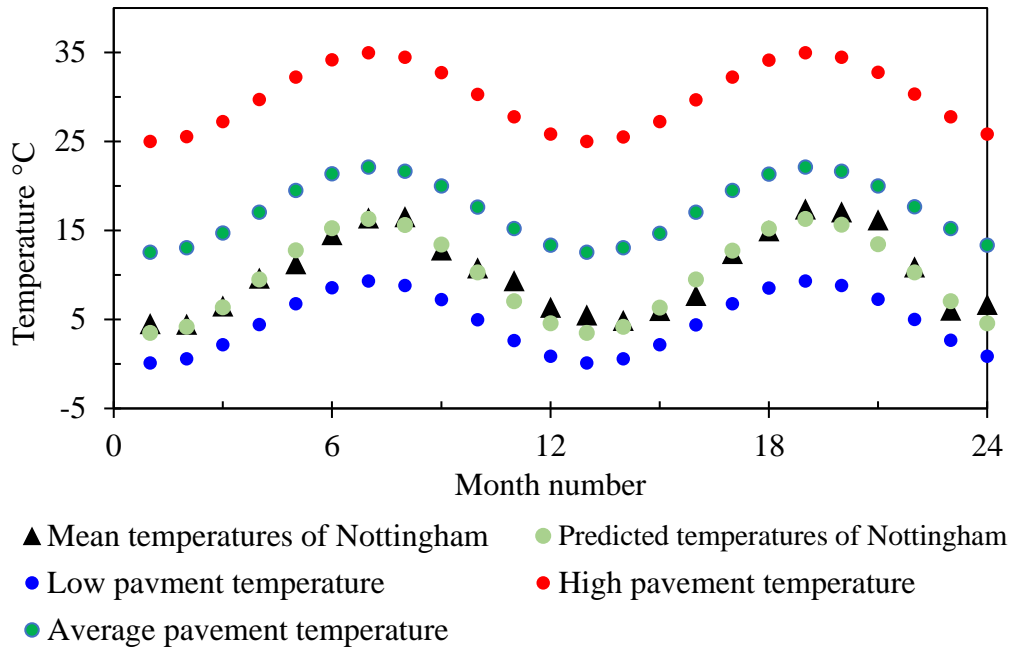
Figure 4. Air and pavement predicted temperatures of the studied area

Traffic Volume

Traffic volume is a critical pavement design parameter (Thom, 2014). Traditionally, the traffic spectrum has been converted to an Equivalent Single Axle Load (ESAL) of 18 kN using load equivalency factors (AASHTO, 1993). Whereas the current MEPDG considers accumulating the structural damage caused by the entire traffic spectrum rather than converting it into ESAL. However, in this case, a significant amount of data is required, and the computational time can be significantly increased. Accordingly, the AAHTO method was considered in this study. To demonstrate the purpose of this study, road A52 located at the west of Nottingham city was considered in this study. Traffic data of this road was downloaded from Department for Transport website (DfT, 2018), then the data were processed in accordance with the recommended traffic assessment method in the UK (DfT, 2006) which resulted in a traffic volume of 162,500 ESAL/ month. Therefore, this volume was considered in this study.

Dynamic Modulus of the Asphaltic Layers

The dynamic modulus is one of the essential fundamental properties of asphaltic materials that is used in the MEPDG to calculate pavement response (Y. R. Kim, et al., 2011). This property can be directly measured by performing dynamic modulus testing. Otherwise, it can be predicted from the mix design and binder properties. In this study, the latter method was adopted. The dynamic modulus was predicted at different temperature and frequencies using the following model (NCHRP, 2004b):

$$\begin{aligned}
\log E^* &= 0.00689 \times [3.750063 + 0.02932 \times \rho_{200} - 0.001767 \times (\rho_{200})^2 - 0.002841 \times \rho_4 \\
&\quad - 0.058097 \times V_a - 0.802208 \times \left(\frac{V_{beff}}{V_{beff} + V_a}\right) \\
&\quad + \frac{3.871977 - 0.0021 \times \rho_4 + 0.003958 \times \rho_{38} - 0.000017 \times (\rho_{38})^2 + 0.005470 \times \rho_{34}}{1 + e^{(-0.603313 - 0.313351 \times \log(f) - 0.393532 \times \log(\eta))}}]
\end{aligned}$$

$$\text{Equation 4}$$

where E^* is dynamic modulus MPa, η bitumen viscosity 10^6 Poise, f loading frequency Hz, V_a air void content %, V_{beff} effective bitumen content %, ρ_{38} cumulative retained on the sieve 19 mm, ρ_{34} cumulative retained on the sieve 9.5mm, ρ_4 cumulative retained on the No. 4 sieve, and ρ_{200} is cumulative retained on the No. 200 sieve. After determining the dynamic modulus at different temperatures and frequencies, a master curve was constructed by the application of the time-temperature superposition principle; then the following generalised logistic function was fitted to the test data since this function was reported to give a proper fitting (M. Kim, Mohammad, & Elseifi, 2015):

13

$$\log(|E^*|) = \delta + \frac{\alpha}{(1 + \lambda \times e^{\beta + \gamma \times \log fr}) \wedge (\frac{1}{\lambda})}$$

Equation 5

where $|E^*|$ is the dynamic modulus, δ is the minimum value of the complex modulus, α is the difference between the minimum and maximum values of the dynamic modulus, and λ, β, and γ are shape parameters. Further details regarding the application of the time-temperature superposition principle and the construction of dynamic modulus master curves can be found elsewhere (Airey, 1997; M. Kim, et al., 2015). The developed master curves for the surface and base layers based on this model are presented in Figure 5. This figure indicates that the base layer has a higher dynamic modulus than the surface layer. This is because a binder grade of 15-25 dmm has been considered for the base layer, and a binder grade of 40-60 dmm has been considered for the surface layer in accordance with British standard BS EN 13108-1 (BSI, 2006).

However, the derived dynamic modulus master curves of the surface and base layers do not take into account the variability associated with this parameter. Because so far, the modulus is calculated as a function of temperature and frequency. But Table 1 indicates that the coefficient of variation of the bituminous layers is 10-20%, which means that the variability associated with this parameter has not yet included in the analysis because the dynamic modulus calculated by equations 3 or 4 is a deterministic value at a specific temperature and frequency. To overcome this issue and to include the variability of the dynamic modulus in the simulation, the calculated modulus at every temperature and frequency was assumed to be the mean value at these conditions, and the standard deviation was calculated accordingly. Then the dynamic modulus that includes the variability was calculated using the following equation:

14

$$E^*_{(T,f)var} = E^*_{(T,f)deter} \times (1 + \frac{CoV}{100} \times RGV)$$

<div align="right">Equation 6</div>

where $E^*_{(T,f)var}$ is the dynamic modulus at a certain temperature and frequency that is randomly generated based on its level of variability, $E^*_{(T,f)deter}$ is the deterministic dynamic modulus determined from the master curves, CoV the coefficient of variance, and RGV is a randomly generated value from the standard Gaussian distribution (mean= 0 and standard deviation=1). Basically, this equation adds the variability associated with the dynamic modulus to the deterministic dynamic modulus calculated from the master curves. Figure 6 shows the dynamic modulus of the surface layer that was developed based on the prescribed method. It can be seen that the modulus varies significantly from one case to another due to the variability associated with this parameter.

Stiffness Modulus of the Unbound Pavement Layers

The stiffness modulus of the sub-base and sub-grade layers were calculated using the following correlation between California Bering Ratio (CBR) and the resilient modulus (NCHRP, 2004c):

$$E_r = 17.6142 \times (CBR)^{0.64}$$

<div align="right">Equation 7</div>

where E_r is the resilient modulus of unbound pavement layers MPa. The CBR values used in this study were assumed to be 35% and 15% for the sub-base and sub-grade layers respectively. Equation 7 does not take into account the variability associated with the sub-base and sub-grade materials. Table 1 shows that the average CoV of the stiffness of these layers is 20%. By using the recommended CoV and assuming that the calculated modulus in Equation 7 is the mean value and by the application of the same concept of Equation 6, Figure 7 and Figure 8 were developed. The

figures show that the modulus of the unbound pavement layers can vary significantly, which can have a significant impact on the prediction of pavement performance.
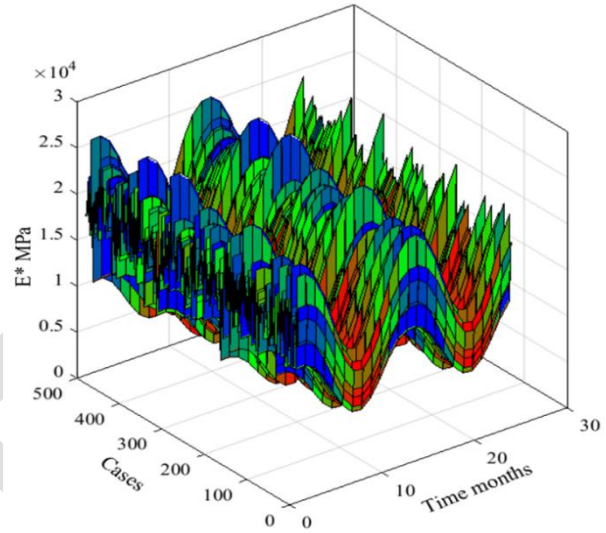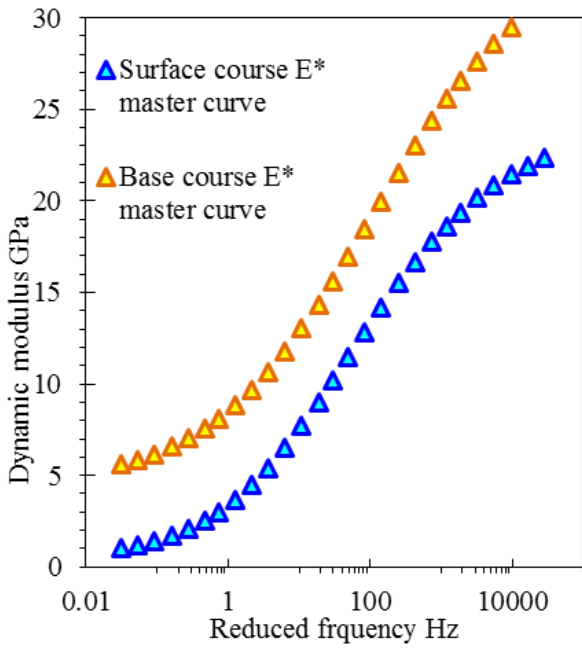

Figure 5. Surface and base layer dynamic modulus master curves

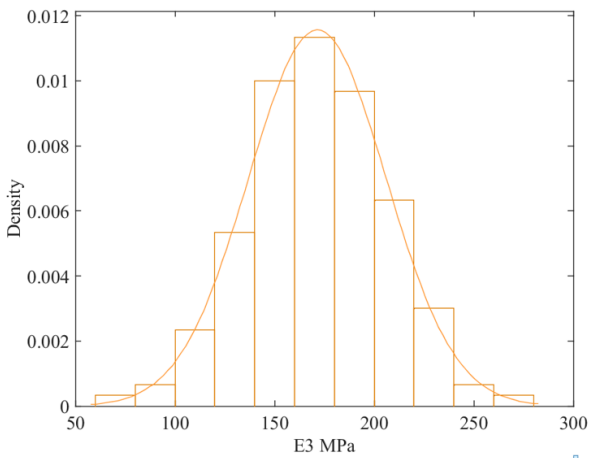Figure 6. Variations of the dynamic modulus

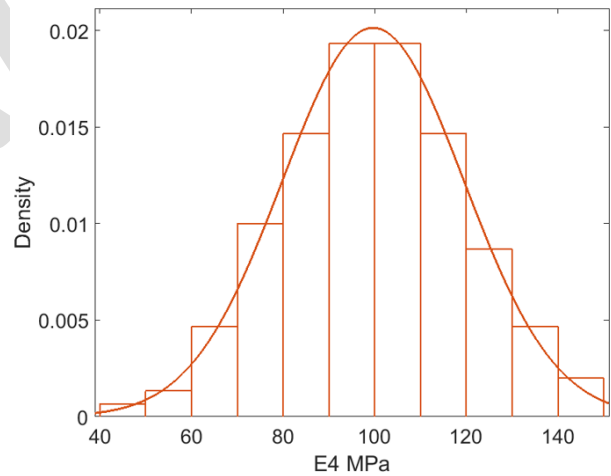Figure 7. Sub-base layer stiffness modulus

Figure 8. Sub-grade layer stiffness modulus

Pavement Response

Pavement performance depends to a significant extent on the way that the pavement responses to

16

the applied stress. Traditionally, pavement response has been calculated based on Burmister's multilayer elastic theory (Huang, 2004). There are several available programmes that can calculate pavement response. Such as KENLAYER, JULEA, and MICHPAVE. These programmes can calculate stresses and strains for multilayer systems. However, to run the simulation, it is required to repeatedly calculate pavement response for thousands of times to obtain an output with a particular distribution which may take a long time to solve one problem. To overcome this issue, KENLAYER was utilised in a novel way to calculate pavement response; it was linked to Matlab software as a subroutine to calculate pavement strain at predefined locations. The Matlab code performs the following procedure to determine pavement response:

(1) It generates random input variables based on each variable's probability distribution.

(2) It determines the average monthly air temperatures then it calculates three pavement temperatures for each month, low and high temperatures, and the average of these.

(3) It calculates the dynamic modulus for the asphaltic layers based on the predetermined temperatures and frequencies. Then it uses Equation 6 to add variability to the calculated modulus based the on recommended CoV in the literature.

(4) Then it sends the generated inputs to KENLAYER programme to calculate pavement response.

(5) Finally, it automatically extracts the analysis results (strains) from KENLAYER at predetermined critical locations to use them in predicting pavement performance.

For bottom-up fatigue cracking, the horizontal critical tensile strain the bottom of the base layer is used to predict the cracking damage. For the rutting, the vertical compressive strain at the middle of each layer is used to predict this distress. For top-down fatigue cracking which initiates at pavement surface, the horizontal tensile strain at pavement surface is in the prediction process. However, most

17

of the available pavement analysis programmes cannot accurately calculate pavement stress and strain near the pavement surface. Huang (2004) demonstrated that KENLAYER resulted in a difference in the calculated tensile strain at analysis depth less than 51 mm in comparison with other software. In other words, KENLAYER was not capable of correctly calculating pavement strains at depths less than 51 mm. JULEA software can calculate pavement response at a minimum depth of 20% of the load contact radius (Khazanovich and Wang, 2007), which means that this software may not accurately calculate pavement response less than that depth. To overcome this issue, an alternative method was followed, the tensile strain at the pavement surface was estimated using the following equation (Thom, 2014):

$$\varepsilon_{surface} = \frac{P}{E} \times \sqrt{6 \times (1 + \upsilon)} \qquad \text{Equation 8}$$

where $\varepsilon_{surface}$ is the shear strain at the edge of the applied load, P is traffic load, E is the stiffness of asphalt layer, and υ is Poisson's ratio. This equation can give a reasonable approximation to the surface tensile strains in an easy computational effort, which makes it suitable for implementation in pavement analysis software.

Fatigue Cracking Performance Prediction

To predict fatigue cracking performance, the MEPDG models (NCHRP, 2004c) were implemented in this study, as follows:

$$FC_{bottom} = \frac{1}{60} \times \frac{6000}{1 + e^{(-2c_2' + c_2' \times \log(D*100))}} \qquad \text{Equation 9}$$

$$FC_{top} = 10.56 \times \frac{1000}{1 + e^{(7.0 - 3.5 \times \log(D*100))}} \qquad \text{Equation 10}$$

where FC_{bottom} is the bottom up cracking (%), FC_{top} is the length of top-down fatigue cracking, c_2'=-2.40874-39.748×(1+hac)^-2.856, and D is the fatigue damage of either bottom up or top down cracking. The primary input to these models is D which was calculated in this study based on Miner's law (Huang, 2004) as follows:

$$D = \sum_{i=1}^{p} \sum_{j=1}^{m} \frac{n_{i,j}}{N_{i,j}}$$

Equation 11

where D is the damage, p is a number of periods, m is number of load groups which equals one in this study since only ESAL was considered in the analysis, $n_{i,j}$ is the predicted load applications, and $N_{i,j}$ is the allowable load application which was calculated based on the Asphalt Institute fatigue life model, as follows (The Asphalt Institute, 1981):

$$FL = C \times K_1 \times \left(\frac{1}{E}\right)^{K_2} \times \left(\frac{1}{\varepsilon_t}\right)^{k_3}$$

Equation 12

where FL is the fatigue life as a number of load applications, $K_1, K_2,$ and K_3 are laboratory regression coefficients, C is a fatigue life laboratory to field shift factor, E is asphalt stiffness, and ε_t is the horizontal strain at the bottom (for bottom-up cracking) or surface (for top-down cracking) of asphalt layer. To sum up, fatigue cracking can be predicted by calculating pavement response (strains) at critical locations under specific loading and environmental conditions, using Equation 12 to calculate fatigue life, determining fatigue damage using Equation 11, then predicting the bottom-up and top-down fatigue cracking using equations Equation 9 or Equation 10 based on the damage location.

19

Permanent Deformation Prediction

Permanent deformation of all pavement layers was predicted using the following model (NCHRP, 2004c):

$$RD = \sum_{i=1}^{number\ of\ sublayers} \varepsilon_p^i \times h_i$$

<div align="right">Equation 13</div>

where RD is total rutting deformation, ε_p^i and h_i are plastic strain and thickness of each sublayer. The plastic strain of the asphaltic layers can be calculated using the following model:

$$\varepsilon_{p,i}^{as} = \varepsilon_{r,i} \times \beta_{r1} \times a_1 \times T^{\beta_{r2}a_2} \times N^{\beta_{r3}a_3} \times k_1$$

<div align="right">Equation 14</div>

where $\varepsilon_{p,i}^{as}$ and ε_r are the plastic and resilient strain of each asphaltic sublayer i, T is the temperature, N is the number of load repetitions, a_1, a_2, a_3 are regressions coefficients, β_{r1} β_{r2} β_{r3} are field calibration factors, and k_1 is a depth parameter to account for confinement pressure in rutting prediction. For the unbound pavement layers, the following model was used:

$$\delta_{p,i} = \beta_1 \times \left(\frac{\varepsilon_0}{\varepsilon_r}\right) \times e^{-\left(\frac{p}{N}\right)^\beta} \times \varepsilon_{v,i} \times h_i$$

<div align="right">Equation 15</div>

where $\delta_{p,i}$ is permanent deformation, β_1 is a calibration factor for unbound and subgrade materials, N is the number of traffic repetition, ε_0, p and β are material properties that can be determined by a resilient test, ε_r the resilient strain used in a resilient modulus test, ε_v is the vertical strain calculated from the pavement response analysis, h_i is the sublayer thickness. To sum up, the permanent deformation can be predicted by calculating the rutting in the asphaltic layers using Equation 14, and in the unbound layers using Equation 15, then the total rutting can be calculated using Equation

13.

Results and Discussion

By applying the derived model, the performance of the studied pavement was simulated for thirty years. To analyse the simulation results, it is critical to fit a distribution that best fits the data so that the reliability of the system can be accurately determined. Therefore, four of the commonly used distributions, Normal, Lognormal, Weibull, and Burr were fitted to the data as shown in Figure 9. Then the distribution that gives the maximum log likelihood was selected, in this case, it was Burr distribution. This distribution has a probability distribution function as follows (MathWorks®, 2015):

$$f(x|\alpha, c, k) = \frac{\frac{k \times c}{\alpha} \times (\frac{x}{\alpha})^{(c-1)}}{(1 + (\frac{x}{\alpha})^c)^{(k+1)}}, x > 0, \alpha > 0, c > 0, k > 0$$

Equation 16

where c and k are the shape parameters, α is the scale parameter, and x is a variable. The shape and scale parameters make this distribution flexible to fit very well different data distributions. Accordingly, this distribution was fitted to the simulation data and utilised to calculate the probability of the simulated stresses. Figure 10, Figure 11, and Figure 12 present the simulation results of the bottom-up fatigue cracking (denoted by FCB_age in years), top-down fatigue cracking (denoted by FCS_age in years), and the total permanent deformation (denoted by PD_age in years) respectively. The results revealed that not only the means of the performance indicators are increasing over time, but the standard deviations are also significantly increasing. This means that the mean distress values are not useful in describing the pavement condition. The probability distribution, however, is a reasonable way to describe the pavement condition due to its capability of predicting the distress at any reliability level. Moreover, the results show that the pavement may

21

fail due to the top down cracking before other distress types appear. This result generally agrees with the common structural performance of the thick pavements in the UK (Thom, Choi, & Collop, 2002).

To further implement the analysis results and to expand the application of the developed simulation tool, the predicted measures were utilised in predicting maintenance time. The MEPDG threshold levels (AASHTO, 2008) (bottom-up fatigue cracking <20% lane area, top-down fatigue cracking <132.6 m/km, Rutting in HMA layers <16.5 mm) for primary highways were applied, and the probability of an output being less than the designated threshold value was calculated from the fitted distributions and presented against the pavement service time, as shown in Figure 13. The results indicate that the pavement will start to exhibit severe top-down cracking between 12-15 years since during this period the probability of being less than the threshold of this distress is dropping. The bottom-up cracking, on the other hand, will never appear even after 30 years of service, since the percentage of the cracking at 30 years is about 2% which is much lower the threshold value of this distress. Regarding permanent deformation, the figure shows that this distress will appear gradually between 15-20 years and after that all simulated cases will exhibit rutting more than 16.5mm. Accordingly, these results can be used in predicting the time to provide maintenance by simply deciding at which probability the maintenance should be provided. For example, if one considers a probability of 0.5 for the top-down cracking as a limit to provide maintenance, then the analysed pavement will need maintenance after 13 years of service.
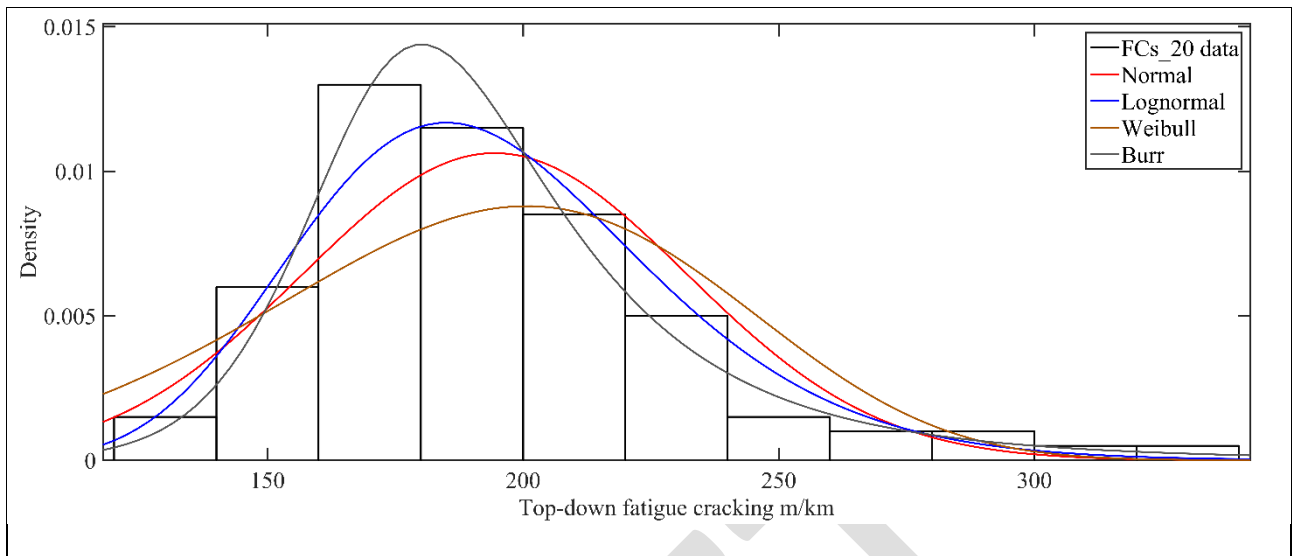
Figure 9. Examining different distributions to best fit simulation data
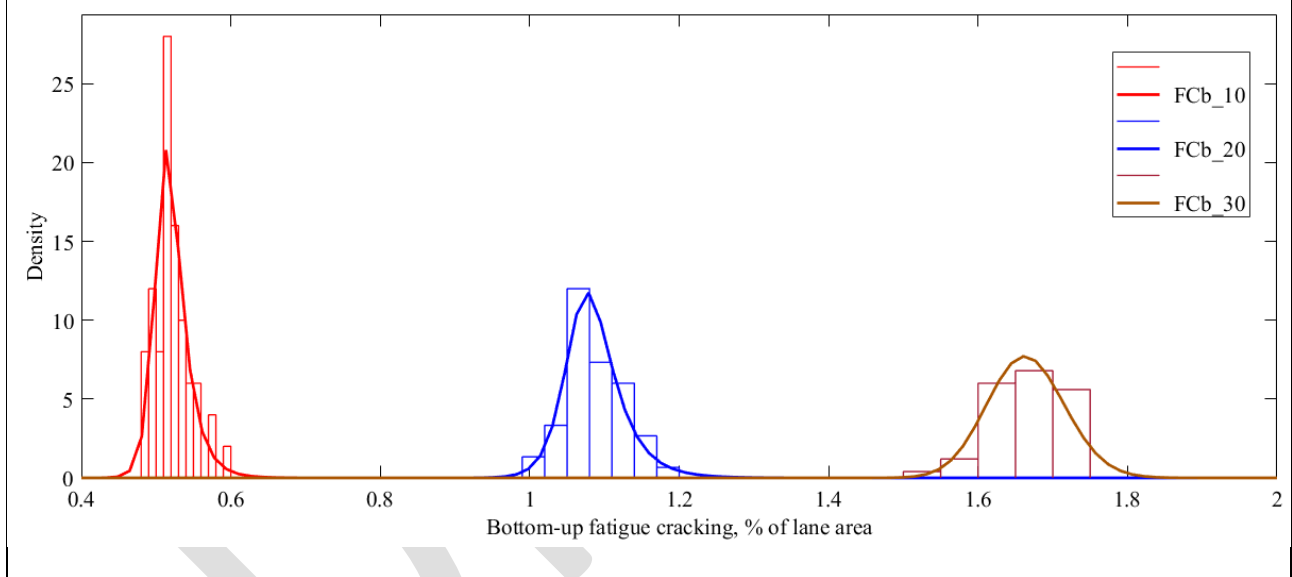

Figure 10. Predicted bottom-up fatigue cracking, % of lane area
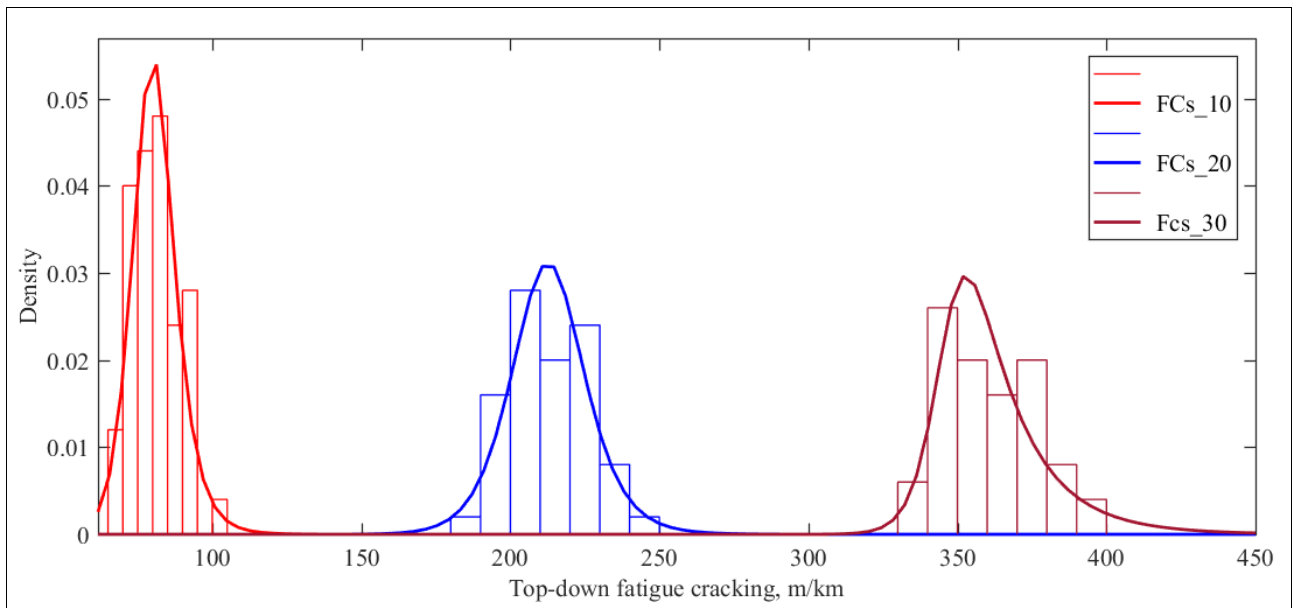
23
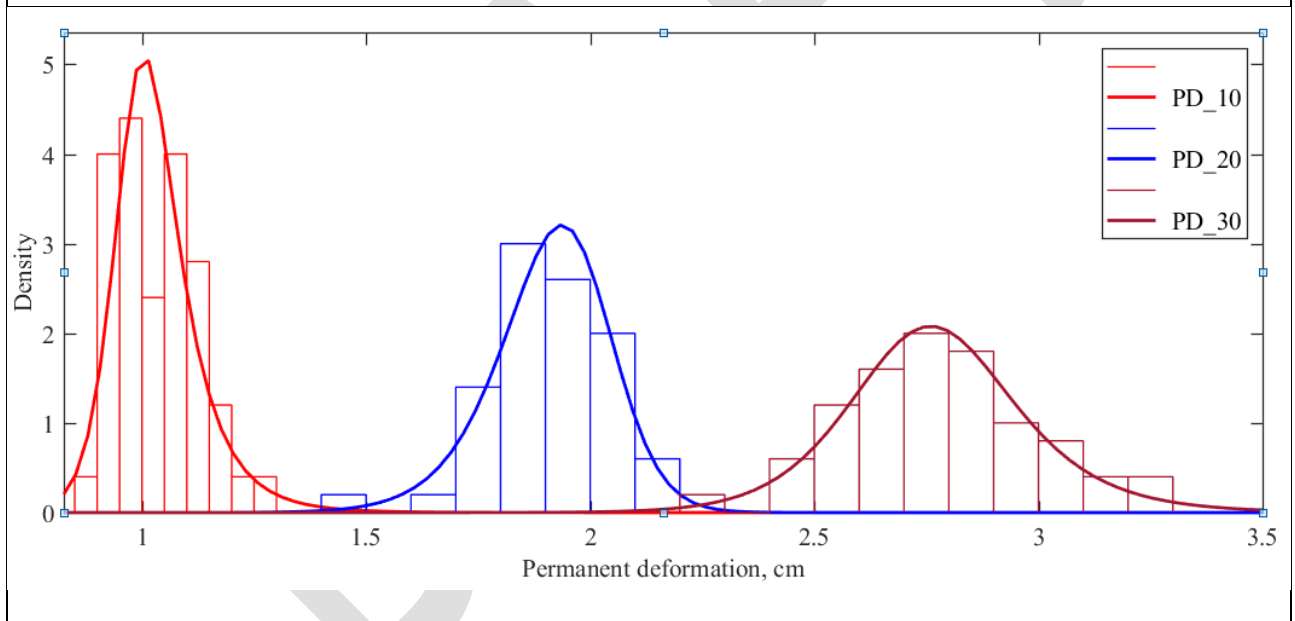
Figure 11. Predicted top-down fatigue cracking, m/km
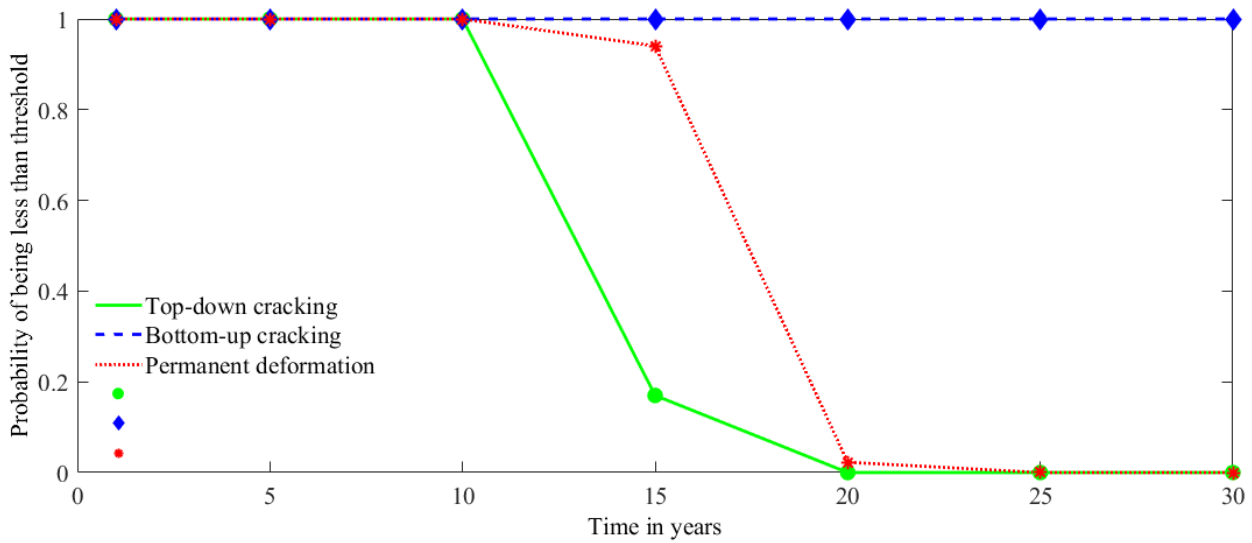

Figure 12. Predicted rutting, cm

Figure 13. The probability of the outputs being less than the threshold values

Number of Simulations

One last critical point to consider is the simulation time. The simulation time depends on two factors, the simulation period and the number of simulations. The former is a user input; it is the aim of the analysis to predict pavement performance after a specified time. Therefore, this factor cannot be used to reduce simulation time. The latter, however, can significantly increase simulation time if it is overestimated, and it may reduce the simulation result if it is underestimated because increasing the number of simulations is expected to improve the efficiency of the simulation process (Ayyub and Klir, 2006). So, this factor must be investigated in order to obtain sufficient simulation results within a reasonable simulation time.

The effect of the number of simulations was studied by running the simulation for different times, such as 50, 75, 100, 125, 150, 250 runs. The statistical significance of each number was then tested against the highest number of runs assuming that this number is sufficient to construct the probability distribution function of the outputs. A two-sample Kolmogorov-Smirnov test was utilised to test the significance. The null hypotheses H_0 of this test is that both samples are from the

25

same distribution; the alternative hypothesis H_1 is that the samples are from different distributions. Following this method, the results of all predicted distress types at a simulation period of 20 years were tested. Interestingly, all the results were insignificantly different from the 250 case, even when a low number of runs such as 50 simulations was considered. This means that this analysis can be successfully performed using only 50 simulations which takes about 3.5 hours to simulate pavement performance for twenty years.

Summary and Conclusions

Variability associated with pavement design parameters has always been a concern to pavement designers and highway agencies. This point becomes even more critical when too many design parameters are involved in the design process, because every parameter may add additional uncertainty to the predicted performance. Therefore, this study aims to address this issue and suggests a framework to probabilistically predict pavement performance and takes into account the variability associated with the design parameters. This aim has been addressed by performing MC simulation. The input parameters were the mean and the standard deviation of the primary pavement design input parameters. KENLAYER was utilised in a novel way to calculate pavement response; it was used as a subroutine with Matlab to determine pavement strains based on the generated inputs by the code. The outputs were the probability distribution functions of the top-down cracking, bottom-up cracking, and permanent deformation. These indicators were calculated by implementing the MEPDG models.

The developed simulation tool was applied to simulate and predict the performance of a typical four-layer asphalt pavement. The pavement was simulated for 30 years, the probability distribution function of the outputs was captured every five years. The simulation results showed that the variability of pavement design inputs has a critical effect on the simulation results. The results also

26

revealed that the probability distribution function of the outputs is expanding, and not only the mean but also the standard deviation is increasing over time. In other words, the mean cannot successfully describe pavement condition, but the probability distribution function which can represent pavement status at any reliability level. Also, it was found that the Burr distribution best fits the predicted distress types and can be used to represent the probability distribution function of these indicators. Furthermore, tracking the probability of distress being less than threshold values over time can be a valuable option to predict pavement maintenance time and the type of the required maintenance. However, the question that remains open in this study is to what probability should roads be maintained?

Limitation: Because the simulation results depend to a significant extent on the models used in the analysis and since these models, unfortunately, were not calibrated to UK weather and material properties, this analysis cannot yet be applied directly to UK roads. The results in the current study are based on specific calibration factors suggested based on the experience of the authors with the analysed pavement system and local material properties. Therefore these factors were not mentioned in the paper to avoid misleading the readers.

Acknowledgements

Disclosure statement

No potential conflict of interest was reported by the authors.

References

1. AASHTO. (1986). AASHTO Guide for Design of Pavement Structures. Washington, D.C., US: American Association of State Highway and Transportation Officials.

2. AASHTO. (1993). AASHTO Guide for Design of Pavement Structures. Washington, D.C., US: American Association of State Highway and Transportation Officials.

3. AASHTO. (2008). American Association of State Highway and Transportation Officials. Mechanistic-Empirical Pavement Design Guide: A Manual of Practice: AASHTO Designation: MEPDG-1. Washington, DC.

4. Abaza, K., & Murad, M. (2007). Dynamic Probabilistic Approach for Long-Term Pavement Restoration Program with Added User Cost. *Transportation Research Record: Journal of the Transportation Research Board, 1990*, pp. 48-56. doi:10.3141/1990-06

5. Abaza, K. A. (2004). Deterministic Performance Prediction Model for Rehabilitation and Management of Flexible Pavement. *International Journal of Pavement Engineering, 5*(2), pp. 111-121. doi:10.1080/10298430412331286977

6. Abaza, K. A. (2014). Back-calculation of transition probabilities for Markovian-based pavement performance prediction models. *International Journal of Pavement Engineering, 17*(3), pp. 253-264. doi:10.1080/10298436.2014.993185

7. Abaza, K. A. (2015). Empirical Approach for Estimating the Pavement Transition Probabilities Used in Non-Homogenous Markov Chains. *International Journal of Pavement Engineering, 18*(2), pp. 128-137. doi:10.1080/10298436.2015.1039006

8. Airey, G. D. (1997). *Rheological characteristics of Polymer Modified and Aged Bitumens* (Doctor of Philosophy PhD). The University of Nottingham.

9. Amador-Jiménez, L. E., & Mrawira, D. (2011). Reliability-Based Initial Pavement Performance Deterioration Modelling. *International Journal of Pavement Engineering, 12*(2), pp. 177-186. doi:10.1080/10298436.2010.535538

10. Ayyub, B. M., & Klir, G. J. (2006). *Uncertainty Modeling and Analysis in Engineering and the Sciences*: Boca Raton, FL, Chapman & Hall/CRC.

11. BSI. (2006). BS EN 13108-1:2006, Bituminous Mixtures - Material Specifications - Part One: Asphalt Concrete. The United Kingdom: British Standards Institution.

12. Butt, A., Shahin, M., Feighan, K., & Carpenter, S. (1987). Pavement Performance Predíction Model Using the Markov Process. *Transportation Research Record 1123*

13. Collop, A., & Cebon, D. (1995) *Modelling Whole-Life Pavement Performance*. Paper presented at the Fourth International Symposium on Heavy Vehicle Weights and Dimensions, Ann, Arbor, USA.

14. Darter, M. I., & Hudson, W. R. (1973). *Probabilistic Design Concepts Applied to Flexible Pavement System Design* CFHR 1-8-69-123-18). Center for Highway Research, The University of Texas at Austin

15. DfT. (2006). *Design Manual for Roads and Bridges, Volume 7: Traffic Assessment*.

16. DfT. (2018). Traffic Counts. Retrieved Date Accessed, 2018 from https://www.dft.gov.uk/traffic-counts/index.php.

17. George, K. P., Rajagopal, A. S., & Lim, L. K. (1989). Models for Predicting Pavement. *Transportation Research Record 1215*

18. Hassan, R., Lin, O., & Thananjeyan, A. (2015). Probabilistic Modelling of Flexible Pavement Distresses for Network Management. *International Journal of Pavement Engineering, 18*(3), pp. 216-227. doi:10.1080/10298436.2015.1065989

19. Huang, Y. H. (2004). *Pavement Analysis and Design* United States of America: Pearson Prentice Hall.

20. Khazanovich, L., & Wang, Q. (2007). MnLayer: High-Performance Layered Elastic Analysis Program. *Transportation Research Record: Journal of the Transportation Research Board*(2037), pp. 63-75.

21. Kim, M., Mohammad, L., & Elseifi, M. (2015). Effects of Various Extrapolation Techniques for Abbreviated Dynamic Modulus Test Data on the MEPDG Rutting Predictions. *Journal of Marine Science and Technology, Vol. 23, No. 3, pp. 353-363 (2015)*doi:10.6119/JMST-014-0327-7

22. Kim, Y. R., Underwood, B., Far, M. S., Jackson, N., & Puccinelli, J. (2011). *LTPP Computed Parameter: Dynamic Modulus* FHWA-HRT-10-035).

23. Li, N., Haas, R., & Xie, W.-C. (1996). Development of a New Asphalt Pavement Performance Prediction Model. *Canadian Journal of civil Engineering, 24*, pp. 547–559

24. MathWorks®. (2015). User's Guide: Burr Type XII Distribution.

25. Mohseni, A. (1998). *LTPP Seasonal Asphalt Concrete (AC) Pavement Temperature Models*.

26. NCHRP. (2004a). *Guide for Mechanistic-Empirical Design of New and Rehabilitated Pavement Structures* 1-37A).

27. NCHRP. (2004b). *Guide for Mechanistic Empirical Design of New and Rehabilitated Pavement Structures: Part 2 Chapter 2: Material Characterisation* Final Report 1-37A). Washington D.C.

28. NCHRP. (2004c). *Guide for Mechanistic Empirical Design of New and Rehabilitated Pavement Structures: Part 3 Chapter 3, Design of New and Reconstructed flexible Pavements* Final Report 1-37A). Washington D.C.

29. The Asphalt Institute. (1981). *Thickness Design Manual (MS-1)* (9th ed.) College Park, Maryland.

30. Thom, N. (2014). *Principles of Pavement Engineering* (Second edition ed.) United Kingdom: ICE Publishing.

31. Thom, N., Choi, Y.-K., & Collop, A. (2002) *Top-down cracking, damage and hardening in practical flexible pavement design*. Paper presented at the Proc 9th International Conference on Asphalt Pavements, Copenhagen.

32. UK Forecast. (2019). UK Weather Services. Retrieved Date Accessed, 2019 from https://www.metoffice.gov.uk/pub/data/weather/uk/climate/stationdata/sheffielddata.txt.

33. Valle, P. D. (2015). *Reliability in Pavement Design* (Doctor of Philosophy. University of Nottingham, United Kingdom.

34. Wang, K., Zaniewski, J., & Way, G. (1994). Probabilistic Behavior of Pavement. *Journal of Transportation Engineering, 120*(3), pp. 358-375.

35. Wu, Z., Yang, X., & Sun, X. (2017). Application of Monte Carlo filtering method in regional sensitivity analysis of AASHTOWare Pavement ME design. *Journal of Traffic and Transportation Engineering (English Edition), 4*(2), pp. 185-197. doi:10.1016/j.jtte.2017.03.006

36. Xiao, X. D. (2012). *Risk Analysis and Reliability Improvement of Mechanistic-Empirical Pavement Design* (Doctor of Philosophy. University of Arkansas, Fayetteville.